Development of a Rapid Response Riverine Oil–Particle Aggregate Formation, Transport, and Fate Model

Lori Jones[1] and Marcelo H. Garcia, Ph.D., Dist.M.ASCE[2]

Abstract: The aftermath of the Kalamazoo River oil spill in 2010, which resulted in years of cleanup efforts, showed that research needs to be done regarding oil–particle aggregate (OPA) formation and transport in riverine environments. Although three-dimensional hydrodynamic models can track the transport of OPAs with a high degree of accuracy, in the event of an oil spill, rapid response is necessary to protect the affected ecosystem and expedite cleanup efforts. In the rapid response model developed in this study, the river hydraulics is one dimensional, and the formation and transport of OPAs are described stochastically via a random walk particle tracking algorithm. Application of the model to the Kalamazoo River in Michigan resulted in estimations of the amount of settled oil, and the location of the centroid of the settled oil, that would be expected for different flow velocities. The main river parameter that influences the formation and subsequent settling of OPAs is the flow velocity, with higher velocities causing more OPA formation and settling rates enhancement because of greater amounts of suspended sediments. **DOI: 10.1061/(ASCE)EE.1943-7870.0001470.**

Introduction

Although petroleum is essential for global operations and daily living, when oil spills happen, they are horrific environmental disasters that take years to restore the damaged ecosystems. Many studies regarding the transport and fate of oil in the event of a spill have been performed for coastal environments (Dalyander et al. 2014; Gustitus and Clement 2017), but studies set in inland water bodies are sparse (Great Lakes Commission 2015; Fitzpatrick et al. 2015a). Inland oil spills are important to study and understand for the purpose of oil spill prevention and response; approximately 60% of all oil spills in the United States are inland (Yoshioka and Carpenter 2002). Additionally, of the large oil spills (oil spills greater than approximately 30,000 L) that have occurred in the United States, approximately 88% were inland spills (Yoshioka and Carpenter 2002). Of these large inland spills, about 60% were from pipelines (Yoshioka and Carpenter 2002). With approximately 260,000 km of oil pipelines running across the United States (DOT 2017), inland oil spills can be expected to continue to be a problem, particularly as pipeline infrastructure ages.

One of the largest inland oil spills in the history of the United States occurred in the Kalamazoo River in Michigan (EPA 2017). Enbridge Line 6B discharged heavy crude oil into the river on July 25, 2010 (EPA 2016; Fitzpatrick et al. 2015b). Oil was still being removed from the river in 2014, 3 years after the spill occurred (Dollhopf et al. 2014). A major reason that oil remains in the river for so long after a spill event occurs is due to oil droplets and sediment particles coagulating and forming oil–particle aggregates (OPAs) (Lee 2002). When particles adhere to the surface of an oil droplet, the density increases, resulting in the greater ability of the OPAs to settle out of the water column (Zhao et al. 2016). By August 2010, only a few weeks after the Enbridge spill, the detection and removal of submerged oil was recognized as a main objective for the cleanup process (EPA 2016). Thus, understanding the hydrodynamic conditions that lead to the oil settling out of the water column into the bed of the river is important to provide technical assistance to the agencies responsible for cleanup efforts in the aftermath of an inland oil spill event (Dollhopf et al. 2014).

There are many complex physical, biological, and chemical processes that occur after oil is spilled into a water body: weathering, spreading, advection, horizontal and vertical dispersion, entrainment, dissolution, emulsification, and sedimentation (Yapa et al. 1994; Gong et al. 2014; Fitzpatrick et al. 2015a). When the oil droplets that form and break off from the main oil plume become entrained into the water column because of turbulent mixing, they mix with sediments in the water and can form the negatively buoyant OPAs (Zhao et al. 2016). Although current riverine oil spill models do not account for the interactions between oil droplets and suspended sediments (Gong et al. 2014), various oil spill models in marine environments have incorporated these effects (Khelifa et al. 2005a, b). Notably, a model developed by Bandara et al. (2011) accounted for the formation of OPAs in a marine environment by using an advection-diffusion equation approach. Additionally, Zhao et al. (2014) developed a numerical model that predicts the transient and steady-state oil droplet size distribution resulting from a mass of spilled oil, called V-DROP. The model uses a population balance equation, with the mechanism of breakup being collisions of the oil with turbulent eddies and the breaking efficiency of the oil droplets being due to turbulent energy and viscous forces (Zhao et al. 2014). The V-DROP model was successfully applied to determine the oil droplet size distribution from mixing due to breaking waves (Zhao et al. 2014). Zhao et al. (2016) developed a numerical population balance model of oil droplets and sediment particles that included a conceptual model of oil–sediment coagulation, called A-DROP. The model describes the formation of OPAs with a collision frequency term and a coagulation efficiency term (Zhao et al. 2016). The coagulation efficiency

[1]Graduate Research Assistant, Ven Te Chow Hydrosystems Laboratory, Dept. of Civil and Environmental Engineering, Univ. of Illinois at Urbana–Champaign, 301 N Mathews Ave., Urbana, IL 61801 (corresponding author). Email: lori2@illinois.edu

[2]Professor and Director, Ven Te Chow Hydrosystems Laboratory, Dept. of Civil and Environmental Engineering, Univ. of Illinois at Urbana–Champaign, 301 N Mathews Ave., Urbana, IL 61801.

Note. This manuscript was submitted on February 28, 2018; approved on June 22, 2018; published online on October 5, 2018. Discussion period open until March 5, 2019; separate discussions must be submitted for individual papers. This paper is part of the ***Journal of Environmental Engineering***, © ASCE, ISSN 0733-9372.

term includes the effects from particles covering the surface of the oil droplet (Zhao et al. 2016), taking into account that the sizes and surface area of the oil and sediment are significant factors in the OPA formation process (Zhang et al. 2010). The A-DROP model was successfully applied to a marine environment domain (Zhao et al. 2016). More recently, important advances had been made regarding the mechanics of oil–particle aggregation in aquatic environments but they have yet to be incorporated into transport and fate models (Zhao et al. 2017).

A previous study of the 2010 Kalamazoo oil spill was conducted that used a three-dimensional hydrodynamic model coupled with a particle tracking algorithm to identify where the OPAs would deposit in Morrow Lake, which is downstream of the spill location (Zhu et al. 2018). With the help of numerical modeling, the study identified under which scenarios OPAs would reach Morrow Lake and the areas of the lake and its delta that would have a high concentration of OPA deposits. This model has the potential to inform decision makers where oil cleanup efforts should be focused in the event of a spill; however, there is a major drawback to this model: the time involved in setting up, calibrating, validating, and running a three-dimensional model. In the event of an oil spill, responding to the emergency as fast as possible is very important to contain the spill and minimize the damage caused to the ecosystem. Thus, it is unreasonable to believe that a three-dimensional model would be used in any capacity in a rapid response scenario. Additionally, the particle tracking algorithm employed by Zhu et al. (2018) used set properties of OPAs, assuming that the oil has already broken into droplets and coagulated with sediments at the beginning of the simulation. This assumption neglects the interactions that the oil has with the sediment during its residence time in the river and thus cannot inform the user under what conditions the oil is more likely to coagulate with suspended sediment nor can predict if OPAs settling rates will decrease as the flow velocity increases along a given river reach.

The main objective of this study is to develop a particle tracking model that describes the formation, transport, and fate of oil droplets and OPAs in a riverine environment after an oil spill has occurred. The simplified model proposed in this study is one dimensional and was developed as a rapid response tool rather than a three-dimensional hydrodynamic model. A one-dimensional model could be quickly applied in the aftermath of an oil spill to determine where to focus cleanup efforts along the river. An additional objective of this study is to use the developed rapid response model to understand where and how much of the oil settles out of the water column at a given time after the spill event. The focus is with how the oil settles out of the water column because the oil that settles onto the sediment of the river bottom is the most difficult to clean in the event of a spill. Much of the analysis performed in this study centered on understanding how different parameters of the riverine environment, such as the mean flow velocity and suspended sediment concentration, affect how much oil settles to the bottom of the river.

Theory

The proposed model in this study contains two fundamental parts: a random walk particle tracking model to transport the oil droplets and OPAs through the riverine environment, and a coagulation model to describe the formation of OPAs during their residence time in the river. Because of the completeness of the A-DROP formulation developed by Zhao et al. (2016), the current study heavily draws on this model to describe the OPA formation. The assumptions made and model development are detailed in the following sections.

Model Assumptions

The one-dimensional model in this study makes several assumptions about the river domain and the oil and sediment particle interactions, and these assumptions are integral to the theory development discussed in this section. Thus, the main assumptions made in this study are as follows:

1. The oil droplets themselves do not break up or adhere to each other. The model accepts an input of the distribution of the oil droplet diameters, and this distribution is treated as the final size distribution of the oil droplets after the initial droplet formation occurred following a spill event (Zhao et al. 2016).
2. When the particles attach to the oil droplet, they cover the oil droplet uniformly and in a monolayer (Zhao et al. 2016). This type of OPA is referred to as a Type 1 OPA, which is characterized by one oil droplet coated with sediment of a smaller diameter (Hayter et al. 2015). There are two other types of OPAs, which are characterized as clumps of multiple small oil droplets with sediments (Hayter et al. 2015), but these OPA types are not considered in this study.
3. Under circumstances of high sediment concentrations and turbulence, OPA breakup has been shown to occur (Zhao et al. 2017). However, this phenomenon is complex and not currently well understood, so in this study it is assumed that, once particles attach to an oil droplet, they do not detach (Zhao et al. 2016).
4. The only type of collisions that result in coagulation are collisions between oil droplets and sediment particles, and OPAs and sediment particles (Zhao et al. 2016). Thus, a collision of an oil droplet and an OPA will not result in coagulation for the purpose of this study.
5. The suspended sediment concentration in the river is assumed to be at a steady, equilibrium state. Thus, sediment particles are not tracked in the model; instead, the suspended sediment concentration is described by a Rouse-Vanoni profile throughout the length of the river (García 2008).
6. Once an OPA settles, it is no longer tracked in the model. Thus, re-entrainment effects of the settled OPAs are not included in the model.
7. The model assumes that the river is a rectangular channel, and the flow is steady and uniform in the longitudinal direction, with constant mean velocity and depth.

Particle Tracking

To simulate the movement of oil droplets and OPAs through the domain, the random walk particle tracking method is used to move the oil through (x, y, z) space (Zhu 2015; Garcia et al. 2013; Visser 1997). The random walk scheme simulates the movement of oil droplets and OPAs through advection and turbulent diffusion. The movements in the longitudinal (x) and lateral (y) directions are given by Garcia et al. (2013)

$$x_{t+\Delta t} = x_t + \left(u + \frac{\partial K_H}{\partial x}\right)\Delta t + R_p\sqrt{2K_H\Delta t} \tag{1}$$

$$y_{t+\Delta t} = y_t + \left(v + \frac{\partial K_H}{\partial y}\right)\Delta t + R_p\sqrt{2K_H\Delta t} \tag{2}$$

where $x_{t+\Delta t}$ and $y_{t+\Delta t} = x$ and y locations of the particle at time $t + \Delta t$; and x_t and $y_t = x$ and y locations of the particle at time t. The longitudinal velocity u and lateral velocity v of the water are

multiplied by the time step (Δt) to account for advection. R_p is a normally distributed random variable with a mean value of zero and a standard deviation of 1 (Visser 1997). K_H is a mean longitudinal and lateral turbulent diffusion coefficient, which can be estimated as (Fischer et al. 1979)

$$K_H = 0.6Hu_* \tag{3}$$

where H = water depth; and u_* = bed shear velocity (García 2008). Since the longitudinal and lateral turbulent coefficients are not dependent on the x and y locations of the particles, the gradient terms in Eqs. (1) and (2) are always equal to zero. The longitudinal velocity u is determined at the location of the particle using the law of the wall, which is given by

$$\frac{u}{u_*} = \frac{1}{\kappa}\ln\left(\frac{u_* z}{\nu}\right) + C_L \tag{4}$$

where κ = von Karman constant (equal to 0.41); z = vertical distance above the bed; ν = kinematic viscosity of the fluid in the channel; and C_L = constant (equal to 5.5 in this study). The shear velocity is determined with Eq. (4) by assuming the average longitudinal velocity occurs at $0.4H$ (Singh 2012).

The vertical movement of the particles in the water column is given by (Zhu 2015)

$$z_{t+\Delta t} = z_t + \left(w - V_s + \frac{\partial K_v}{\partial z}\right)\Delta t + R_p\sqrt{2K_v\Delta t} \tag{5}$$

where $z_{t+\Delta t} = z$ location of the particle at time $t + \Delta t$; $z_t = z$ location of the particle at time t; w = vertical velocity of the fluid in the domain; V_s = fall velocity of the particle; and K_v = vertical eddy diffusivity, given by (Van Rijn 1984)

$$K_v = \beta_T \upsilon_T \tag{6}$$

where υ_T = fluid eddy viscosity; and β_T = dimensionless factor used to describe the difference in the diffusion of an oil droplet or OPA and a fluid particle. β_T is given by (Van Rijn 1984)

$$\beta_T = 1 + 2\left[\frac{V_s}{u_*}\right]^2 \tag{7}$$

The fluid eddy viscosity is described by a parabolic-constant profile given by the following relation (Van Rijn 1984):

$$\upsilon_T = \begin{cases} 0.25\kappa u_* H & \text{for } \dfrac{z}{H} > 0.5 \\ \kappa u_* z\left(1 - \dfrac{z}{H}\right) & \text{for } \dfrac{z}{H} < 0.5 \end{cases} \tag{8}$$

The partial derivative of the vertical eddy diffusivity with respect to the vertical direction z, $\partial K_v/\partial z$, is approximated with a central finite-difference scheme except for when the particle is at the water surface (in which case a backward difference scheme is used) or the bottom of the river (in which case a forward difference scheme is used).

Fall Velocity Calculations

The settling velocity of the OPAs is determined by (Zhao et al. 2016)

$$V_{s,\mathrm{OPA}} = \sqrt{\frac{4g(\rho_{\mathrm{OPA}} - \rho_w)D_{\mathrm{OPA}}}{3C_D\rho_w}} \tag{9}$$

where g = acceleration of gravity; ρ_{OPA} = density of the OPA; ρ_w = density of the fluid; D_{OPA} = diameter of the OPA; and C_D = drag coefficient. Eq. (9) results from a force balance of the gravitational, buoyancy, and drag forces working on the OPA. The drag coefficient depends on the Reynolds number of the OPA; the Reynolds number and drag coefficient relationships are given by (Zhao et al. 2016)

$$\mathsf{R}_{\mathrm{OPA}} = \frac{V_{s,\mathrm{OPA}}D_{\mathrm{OPA}}}{\nu} \tag{10}$$

$$C_D = \begin{cases} \dfrac{24}{\mathsf{R}} & \text{for } \mathsf{R} < 1 \\ \dfrac{24}{\mathsf{R}} + \dfrac{3}{\sqrt{\mathsf{R}}} + 0.34 & \text{for } 1 < \mathsf{R} < 10{,}000 \\ 0.4 & \text{for } \mathsf{R} > 10{,}000 \end{cases} \tag{11}$$

Eqs. (9)–(11) are solved iteratively until the settling velocity does not significantly change in two successive iterations. The formulation of the terminal velocity of the oil droplets accounts for how the shape of the droplets change with the diameter (Zheng and Yapa 2000). The terminal velocity is calculated by using Eq. (12), where the Reynolds number is given by the following relationship in Eq. (13) (Zheng and Yapa 2000):

$$V_{s,\mathrm{oil}} = \frac{\mathsf{R}_{\mathrm{oil}}\nu}{D_{\mathrm{oil}}} \tag{12}$$

$$\begin{aligned} &\mathsf{R}_{\mathrm{oil}} = \frac{N_D}{24} - 1.7569\times10^{-4}N_D^2 + 6.9252\times10^{-7}N_D^3 - 2.3027\times10^{-10}N_D^4 && \text{for } N_D \le 73 \\ &\log(\mathsf{R}_{\mathrm{oil}}) = -1.7095 + 1.33438W - 0.11591W^2 && \text{for } 73 < N_D \le 580 \\ &\log(\mathsf{R}_{\mathrm{oil}}) = -1.81391 + 1.34671W - 0.12427W^2 + 0.006344W^3 && \text{for } N_D > 580 \end{aligned} \tag{13}$$

In Eq. (13), $W = \log(N_D)$ and $N_D = [4\rho_w(\rho_w - \rho_{\mathrm{oil}})gD_{\mathrm{oil}}^3]/3\mu^2$, where μ is the dynamic viscosity of the fluid.

Suspended Sediment Concentration

When the oil droplets come into contact with sediment particles, there is a probability that the oil and sediment will coagulate, forming an OPA (Waterman and Garcia 2015). The suspended sediment concentration within the domain is assumed to be at steady state, only varying with the vertical direction. Thus, instead of implementing particle tracking for the sediment particles, the model solves for the distribution of sediment in the river at steady, equilibrium state and uses the concentration of sediment at a given location to compute the coagulation probability. The distribution

of suspended sediment in the water column is described by a Rouse-Vanoni profile (Rouse 1939). The Rouse-Vanoni profile is given by (García 2008)

$$\frac{C}{C_b} = \left[\frac{(1-\zeta)/\zeta}{(1-\zeta_b)/\zeta_b}\right]^{\frac{V_{sed}}{\kappa u_*}} \tag{14}$$

where C = volume concentration of suspended sediment at a given location z in the water column; C_b = near-bed concentration of sediment; $\zeta = z/H$ where H is the water depth; $\zeta_b = z_b/H$ where z_b is the location where C_b occurs; and V_{sed} = fall velocity of the sediment. The fall velocity of the sediment is calculated by using the following formulation (Dietrich 1982)

$$V_{sed} = R_f\sqrt{RgD_{sed}} \tag{15}$$

where R = submerged specific gravity of the sediment (equal to 1.65 in this study); and D_{sed} = diameter of the sediment. R_f is an empirically determined relationship given by (Dietrich 1982)

$$\mathrm{R}_f = \exp\{-2.891394 + 0.95296\ln(\mathrm{R}_p) - 0.056835[\ln(\mathrm{R}_p)]^2 - 0.002892[\ln(\mathrm{R}_p)]^3 + 0.000245[\ln(\mathrm{R}_p)]^4\} \tag{16}$$

where R_p = Reynolds number of the sediment particle, given by (Dietrich 1982)

$$\mathrm{R}_p = \frac{\sqrt{RgD_{sed}}D_{sed}}{\nu} \tag{17}$$

The near-bed equilibrium volumetric concentration of the sediment, C_b, which is assumed to occur at $z_b = 0.05$ (García and Parker 1991), is calculated with the Wright-Parker entrainment relation, given by (Wright and Parker 2004)

$$C_b = \frac{AZ^5}{1 + \frac{A}{0.3}Z^5} \tag{18}$$

where $A = 7.8 \times 10^{-7}$; and Z is given by (Wright and Parker 2004)

$$Z = \left[\frac{u_{*s}}{V_{sed}}f(\mathrm{R}_p)\right]S^{0.08} \tag{19}$$

where u_{*s} = shear velocity multiplied by the square root of the fraction of shear stress that is skin friction if bedforms are present. In this study, it is assumed that dunes and ripples are absent; hence, the fraction of shear stress that is skin friction is assumed to be equal to 1, so $u_{*s} = u_*$. $f(\mathrm{R}_p)$ is a function of the sediment particle's Reynolds number given by García and Parker (1993) and Wright and Parker (2004):

$$f(\mathrm{R}_p) = \begin{cases} \mathrm{R}_p^{0.6} & \text{for } \mathrm{R}_p \le 233.7 \\ 26.38 & \text{for } \mathrm{R}_p > 233.7 \end{cases} \tag{20}$$

Oil–Particle Coagulation

Collision Frequency

The probability of coagulation between an oil droplet and a sediment particle is assumed to be described by a collision frequency term and a coagulation efficiency term (Zhao et al. 2016). The collision term (β) accounts for collisions between two spherical particles with diameters of D_i and D_j due to turbulent shear and differential settling (Zhao et al. 2016)

$$\beta = \beta_{sh} + \beta_{ds} \tag{21}$$

An additional collision term for Brownian motion can be included in the preceding relationship, but Brownian motion is only a pertinent collision mechanism for very small particles (less than 1 μm) (Zhao et al. 2016). The particles considered in this study (the oil droplets, OPAs, and sediment particles) are at least an order of magnitude larger than 1 μm, so Brownian motion is considered to be negligible and therefore not included in the collision frequency term. The turbulent shear mechanism of collision is given by (Zhao et al. 2016)

$$\beta_{sh} = \frac{1}{6}(D_i + D_j)^3\sqrt{\frac{\varepsilon}{\nu}} \tag{22}$$

where ε = energy dissipation rate. The following equation is used to determine the value of ε as a function of the position within the water column (Nezu 2005)

$$\frac{\varepsilon H}{u_*^3} = 9.8\left(\frac{z}{H}\right)^{-1/2}\left[\exp\left(-3\frac{z}{H}\right)\right] \tag{23}$$

The differential settling collision mechanism is given by (Zhao et al. 2016)

$$\beta_{ds} = \frac{\pi}{4}(D_i + D_j)^2|V_{si} - V_{sj}| \tag{24}$$

where V_{si} and V_{sj} = fall velocities of the particles with diameters of D_i and D_j, respectively.

Coagulation Efficiency

Not every collision between an oil droplet or OPA and a sediment particle will result in successful coagulation. The ratio of the amount of successful coagulation events to the total number of collisions is given by the parameter α (Zhao et al. 2016)

$$\alpha(t) = \alpha_{sta}\left(1 - \frac{\sum N(D_{sed}, t)\frac{1}{4}\pi D_{sed}^2}{F_{SP}\pi D_{\mathrm{oil}}^2}\right) \tag{25}$$

where α_{sta} = stability ratio; $N(D_{sed}, t)$ = number of sediment particles already attached to a given OPA at a given time t; D_{sed} = diameter of the attached sediment particles; D_{oil} = diameter of the oil droplet on which the sediment particles are attached; and F_{SP} = factor that accounts for the effects that particle shape and packing has on coagulation. The stability ratio describes the amount of successful coagulation events to the total number of collisions before any sediment particles are attached to an oil droplet. The portion of Eq. (25) in parentheses accounts for decreased coagulation efficiency as more sediment particles adhere to the surface of the oil droplet. The stability ratio is formulated on the basis of a free-energy analysis (Zhao et al. 2016)

$$\alpha_{sta} = \exp\left(\frac{1}{\Delta F}\right) \quad \text{for } \Delta F < 0 \tag{26}$$

where ΔF = dimensionless term that describes the change in free energy per unit surface area of a particle per unit interfacial tension between oil and water

$$\Delta F = \left(\frac{D_m^2 - D_{\mathrm{oil}}^2}{D_{sed}^2}\right) - N_{phex}\frac{1}{4}\sin^2\theta + N_{phex}\frac{1}{2}(1 - \cos\theta)\cos\theta \tag{27}$$

where θ = three-phase contact angle (between the oil droplet, the sediment particle, and the surrounding fluid), which is assumed to

be 60° is this study; and D_m = size of an OPA when the maximum number of sediment particles are attached. The maximum number of sediment particles that can attach is given by N_{phex}. D_m and N_{phex} are given by (Zhao et al. 2016)

$$D_m^3 = D_{\text{oil}}^3 + N_{phex}\frac{D_{sed}^3}{4}(1-\cos\theta)^2(2+\cos\theta) \tag{28}$$

$$N_{phex} = \frac{2\pi}{\sqrt{3}}\left(\frac{D_m + D_{sed}\cos\theta}{D_{sed}}\right)^2 \tag{29}$$

Eqs. (28) and (29) are solved iteratively to get the values of D_m and N_{phex}. The following relation determines how many sediment particles attach to an oil droplet at any given time:

$$\Delta N_p(t) = \alpha(t)\beta N_{sed} \tag{30}$$

where $\Delta N_p(t)$ = change in sediment particles attached to the oil droplet at time t; and N_{sed} = number of sediment particles at the oil droplet or OPA's location in the river, given by the Rouse-Vanoni profile [Eq. (14)].

OPA Volume

Assuming the sediment particles coat the surface of the oil droplet uniformly when they attach, the maximum possible volume of an OPA is given by (Zhao et al. 2016)

$$V_{\text{OPA,max}} = \frac{\pi}{6}(D_m + D_{sed}\cos\theta)^3 + \frac{\pi}{12}N_{phex}D_{sed}^3 \tag{31}$$

A linear relationship between the volume of an OPA and $V_{\text{OPA,max}}$ is used, which is described by (Zhao et al. 2016)

$$V_{\text{OPA}} = V_o + (V_{\text{OPA,max}} - V_o)\frac{N_p}{N_{phex}} \tag{32}$$

where V_o = volume of the oil droplet; and N_p = number of sediment particles attached to the oil droplet.

Boundary Conditions

To ensure no oil droplets or OPAs are transported outside of the domain of the river, the model implements boundary conditions for the water surface, the bottom of the river, and the sides of the river. If the particle hits the sides of the river or is transported outside of the width of the river, then it is considered to have settled onto the banks of the river. Thus, the particle's position is fixed to the river bank and is no longer tracked within the model.

For the water surface, if a particle is transported above the water surface, then the particle is simply fixed at the elevation of the water surface (i.e., floating oil). A reflective boundary condition is not appropriate for the water surface because the oil droplets are positively buoyant before they coagulate with a sediment particle, so a reflective boundary condition would result in artificial submergence of the oil. For the bottom of the river, if an OPA hits the bottom or is transported to a position below the bottom, it is considered settled. Thus, the OPA's position is fixed to the point where it settled for the rest of the simulation. This boundary condition, along with the boundary condition of the river banks, will be updated when more knowledge about the entrainment of OPAs from a sediment bottom becomes available.

Model Validation

Experimental data of the transport and formation of OPAs in a riverine environment are practically nonexistent in the current literature; thus, a straightforward validation of the proposed model could not be performed. However, the proposed model consists of two fundamental parts: particle tracking in a uniform, steady-flow domain, and the formation of OPAs. To validate the model, these two processes are validated independently to demonstrate that the model accurately captures both phenomena.

Validation of Particle Tracking Algorithm

To validate the particle tracking component of the model, modeling results were compared to the results of flume experiments conducted by Tang et al. (1989) with carp eggs. This data set was used for validation because it provides an example of discrete particles traveling in a uniform, steady-flow domain and was used to successfully validate a previously developed particle tracking model (Garcia et al. 2013). The vertical distribution of particles in the water column reported by Tang et al. (1989) and the model results are compared for four different mean flow velocities (0.4, 0.3, 0.25, and 0.2 m/s). The diameter and density of the carp eggs used in the experiments were 4.2 mm and 999.78 kg/m^3, respectively (Tang et al. 1989; Garcia et al. 2013). The experimental flume was 30 m long and 0.72 m wide and had a water depth of 0.6 m (Tang et al. 1989; Garcia et al. 2013). To simulate all four cases, the model introduced the particles at the water surface, midway along the width of the flume. The model used a simulation time of a half hour, after which it was found that the vertical distribution of the particles does not change significantly.

The comparison of the model results and experimental results of Tang et al. (1989) are shown in Fig. 1. The x-axis is the vertical concentration of particles at a specific vertical location divided by the average concentration of the particles (C_z/C), and the y-axis is the vertical location normalized to the flow depth (z/H). For an average flow velocity of 0.2 m/s, there is good agreement between the model and experimental results. For the higher velocities of 0.4, 0.3, and 0.25 m/s, the model tends to underestimate the number of particles in the upper part of the water column, and slightly overestimate the number of particles in the lower part of the water column. A possible source of this discrepancy is the uncertainty of the measurements made by Tang et al. (1989); the flow velocity used in the experiments was measured from a single cross section near the egg sampling device, and the accuracy of the measurement was not reported (Garcia et al. 2013). It is possible that the flow within the flume varied spatially, and this was not captured by the single measurement taken. However, although the model does not capture the exact vertical distribution reported by the Tang et al. (1989) experiments, the same trend in the shape of the distribution with varying flow velocities is captured, with a more uniform distribution for faster flows and a more slanting distribution for lower flows. Additionally, for the three higher velocities, the modeled mean of the vertical distribution ($C_z/C = 100$) matches very well with the experimental mean of the vertical distribution. Thus, this validation exercise shows that the particle tracking algorithm of the proposed model in this study captures the expected trend of the vertical distribution of particles with different flow velocities and does a good job at capturing the vertical centroid of the particles.

Validation of OPA Formation

To validate the OPA formation process of the model presented in this study, modeling results were compared to the same set of experimental results from Sun et al. (2010) that the modeling results of the A-DROP model, developed by Zhao et al. (2016), was compared to. In the study by Sun et al. (2010), Arabian medium

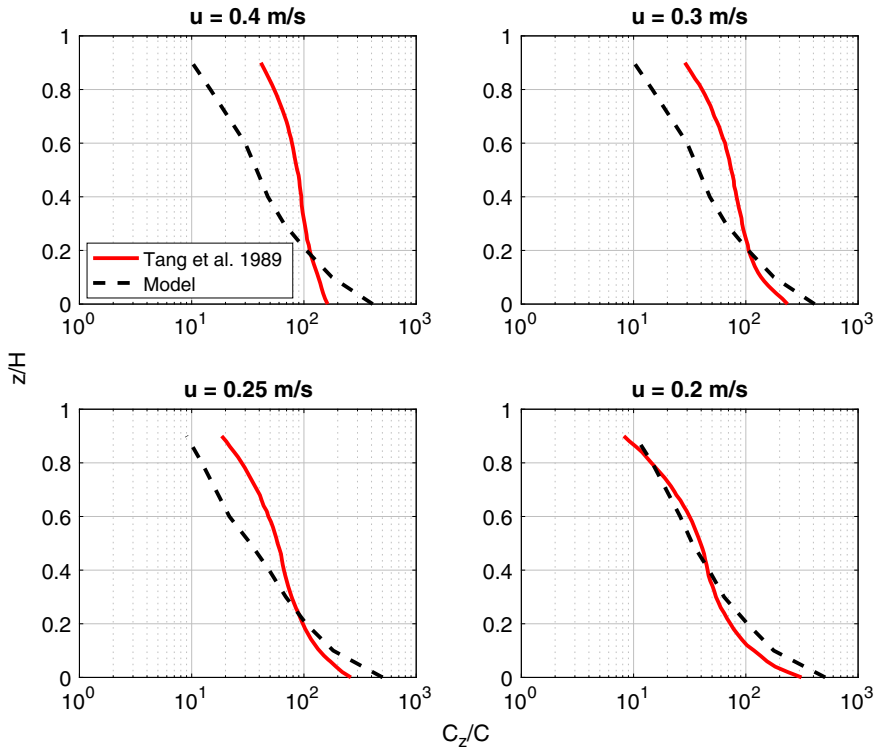

Fig. 1. Comparison of the vertical particle distribution generated with the model and from experimental carp egg flume experiments conducted by Tang et al. (1989).

crude oil (which has a density of 880.9 kg/m^3) was mixed with the standard reference material SRM-1941b (which has a density of 2,570 kg/m^3) in artificial seawater (Sun et al. 2010). The median grain size of the SRM-1941b sediment was approximately 5.3 μm (Sun et al. 2010). The experiments were performed in an Erlenmeyer flask using a reciprocating shaker to simulate mixing, with three different sediment concentrations (100, 200, and 400 mg/L) (Sun et al. 2010). The experiments done with a shaking rate of 2.1 Hz, which corresponds to an energy dissipation rate of 2.6 W/kg (Zhao et al. 2016), were used for the validation exercise. The same oil droplet size distribution used in the A-DROP model validation was used in this study (Fig. 2) (Zhao et al. 2016). The comparison of the model results with the experimental data is shown in Fig. 3.

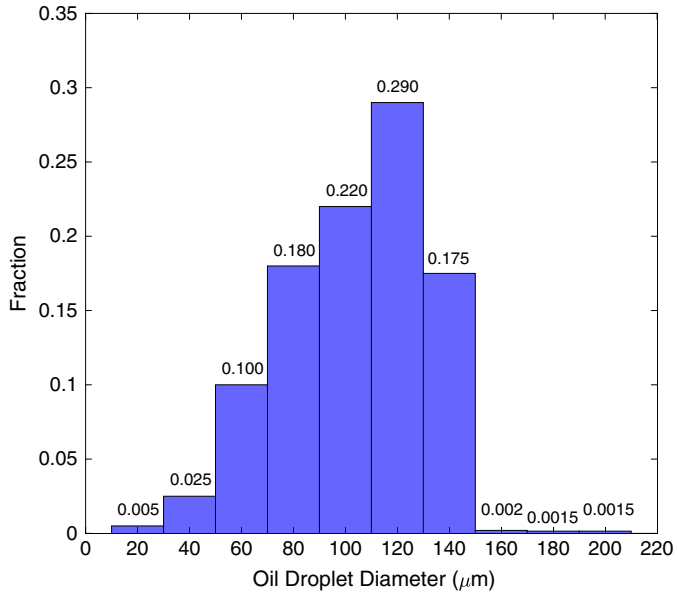

Fig. 2. Oil droplet distribution, determined by Zhao et al. (2016) for the validation of the A-DROP model, used for the validation of the OPA formation process of the model.

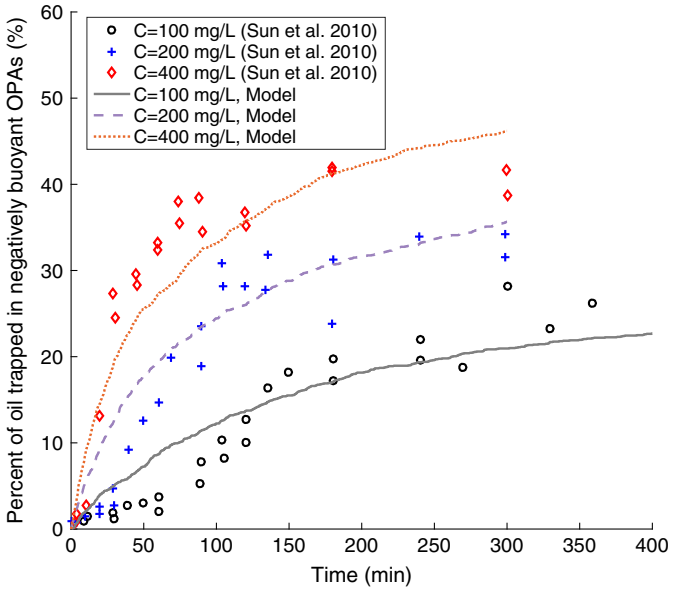

Fig. 3. Comparison of the model results with the experimental data of Sun et al. (2010).

For the sediment concentrations of 100 and 200 mg/L, the model tends to overestimate the amount of OPAs in the first 100 min. This is likely due to the inherent transport differences of the model and the experiments. In the model, the oil droplets are transported in riverine-like conditions, with a velocity distribution that varies with the vertical location of the oil droplet within the water column. The velocity distribution means that the oil droplets that are deeper within the water column are moving less than the oil droplets near the surface, giving these deeper oil droplets less chances to collide and coagulate with sediments. This is unlike the shaker experiments, in which the oil droplets can be assumed to move within the flask approximately the same way, no matter the depth. This may explain the tendency for OPAs to form faster in the model than in the experiments, since oil droplets are introduced at the water surface.

Another difference in the model versus the experimental data is that, with sediment concentrations of 200 and 400 mg/L, the experimental data reach an equilibrium of the number of OPAs formed, whereas the model results show that an equilibrium point has not been reached in the same amount of time. In the experiments, as OPAs form, the concentration of the sediment not aggregated with any oil droplets necessarily decreases within the flask, since the amount of sediment introduced is finite. In the model, the concentration of the sediment is not affected by OPA formation, since the oil droplets and OPAs are moving to a new location in each time step, and there is effectively an infinite source of sediment in the river (since the sediment is entrained from the bed). Thus, the reduction in the chances of collision and coagulation that is experienced by the oil droplets in the experiments is not replicated in the model, accounting for this difference. Despite these differences, overall, the results of the OPA formation in the model follow the same trends for the three different sediment concentrations as the experiments by Sun et al. (2010). This validation exercise shows that the modeled OPA formation process gives expected results for applying the oil droplet–sediment collision and coagulation process to a riverine environment.

Data Input and Parameters

Oil Parameters

The model in this study accepts user input of the distribution of oil droplet sizes; the model does not include breakup of the oil itself. Thus, the input of the oil droplet sizes is assumed to be the steady-state distribution of the oil droplets after an initial spill of oil has occurred. The distribution of oil droplet sizes used in this study is shown in Fig. 4; 1,000 oil droplets are used in each simulation.

In addition to the initial oil droplet size distribution, the density of the oil is also input into the model. In this study, three different types of oil are investigated (Table 1). These types of oil were chosen for this study to serve as examples of low-, medium-, and high-density oils. This range of oil density is used to explore the relationship the density of the oil has on the affinity for the oil droplets to form OPAs and settle out of the water column.

River Parameters

The river in this model is described as a simple rectangular flume with uniform flow conditions. The model accepts input of the average longitudinal (u), lateral (v), and vertical (w) velocity components; the flowrate (Q); the flow depth (H); and the slope (S). Six scenarios, indicative of increasingly faster flows, were tested in this study, and the parameters of these five cases are shown in Table 2.

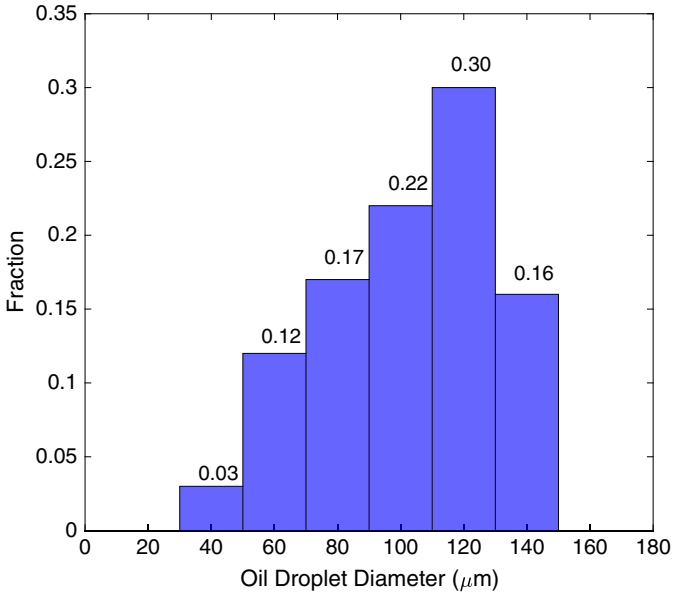

Fig. 4. Initial distribution of the oil droplet sizes.

In addition to the parameters describing the flow in the river, the diameter of the sediment in the river is also an input. The sediment is assumed to be uniform, and in this study the sediment size is assumed to be 50 μm. Each simulation is performed for a simulation time of 5 h. Additionally, the oil is introduced at the surface ($x = 0$ m; $z = 3$ m), midway along the y-direction of the river. In all of the cases described in Table 2, the river is 100 m wide, so the oil is introduced at $y = 50$ m.

Courant Condition

The time step used in the model is user defined, and the results of the model are sensitive to the choice of time step. The sensitivity to the time step is caused by the way the probability of collision and coagulation of an OPA or oil droplet and sediment particle is calculated. The Rouse-Vanoni equilibrium sediment concentration profile provides the volume concentration of sediment at a given point in the river [Eq. (14)]. As the OPA or oil droplet travels in the x-, y-, and z-directions, the average concentration of

Table 1. Three different types of oil used in the current study

Type of oil	Density (kg/m^3)
South Louisiana crude oil (Zhao et al. 2016)	820
Silicon oil (Zhao et al. 2014)	968
Benzene-carbon tetrachloride (Zhao et al. 2014)	1,000

Table 2. River parameter input for the three scenarios tested in this study

u (m/s)	v (m/s)	w (m/s)	Q (m^3/s)	H (m)	S
0.2	0	0	60	3	0.001
0.3	0	0	90	3	0.001
0.4	0	0	120	3	0.001
0.5	0	0	150	3	0.001
0.6	0	0	180	3	0.001
0.7	0	0	210	3	0.001

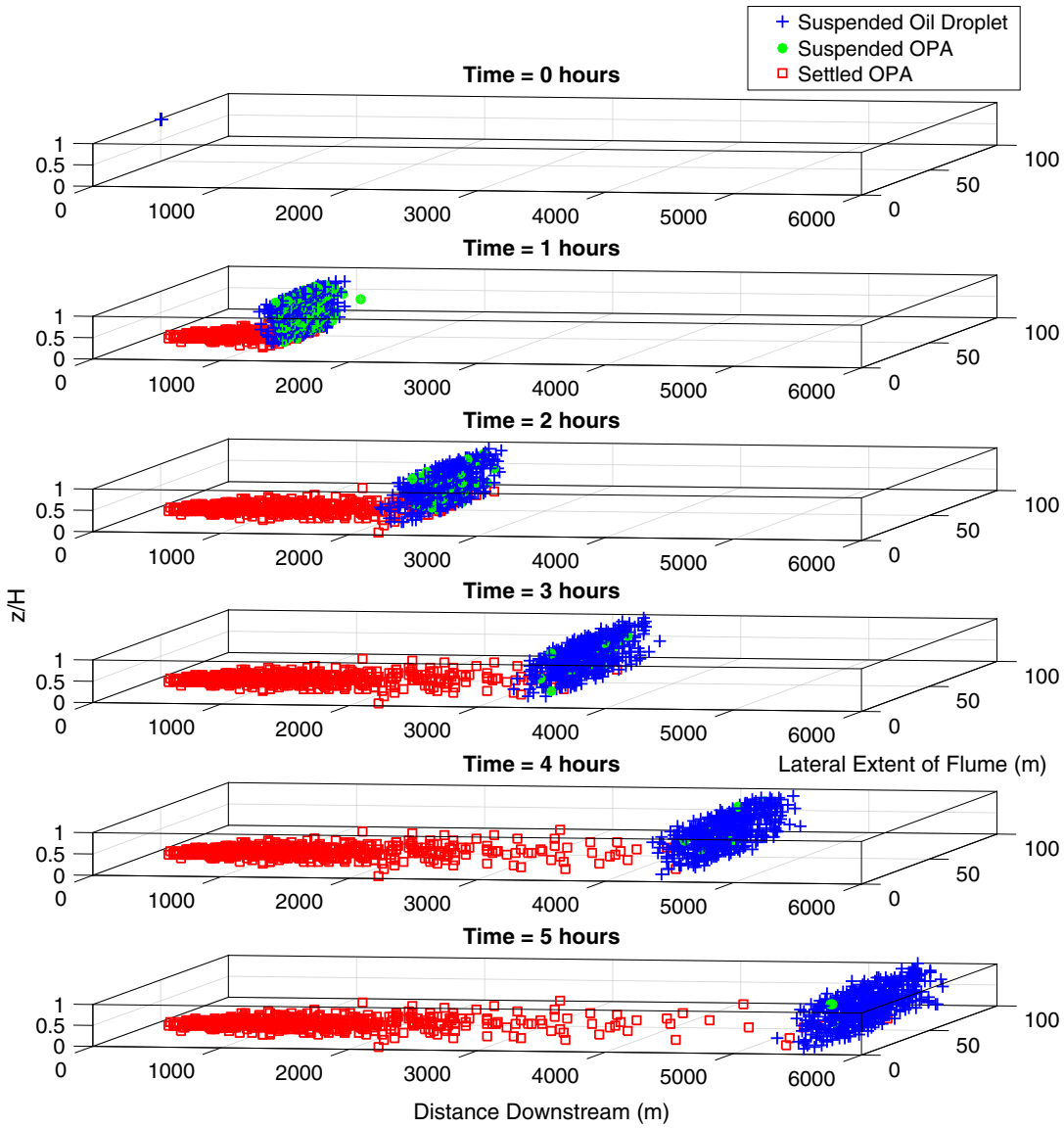

Fig. 5. Snapshots in time of the oil droplets and OPAs in the river domain using South Louisiana crude oil and a flow velocity of 0.5 m/s.

sediment in the volume of water that the OPA or oil droplet travels through in the given time step is used to calculate the number of sediment particles that can interact with an OPA or oil droplet. Thus, increasing the time step results in the OPA or oil droplet traveling a greater distance within that time step, which increases the number of sediment particles that the OPA or oil droplet can interact with, resulting in increased coagulation. Therefore, a limit on the time step is proposed in the form of a courant number, given by

$$Co = \frac{u\Delta t}{L} \tag{33}$$

where Co = Courant number; u = longitudinal velocity; Δt = time step; and L =characteristic length of the river. For this study, the Courant number is set to a value of 1, and the characteristic length of the river is chosen as the depth of the flow. Thus, with an increase in longitudinal velocity in the river (and keeping the flow depth the same), the time step used in the computations decreases.

Results and Discussion

Visualization of How the Model Works

Before discussing results and findings of different model simulations, a visualization of the particle tracking method applied in this model is shown in Fig. 5. This figure shows an example of snapshots through time of the oil droplets and OPAs within the domain for the South Louisiana crude oil, 0.5-m/s flow velocity case.

Simulation Results

For the three different oil densities simulated, the percentage of the total introduced oil that settled at the end of the 5-h simulation time is recorded for each velocity in Table 3. The location of the mass centroid of the settled oil for each case is also listed in Table 3. For all three oil densities, the percentage of settled oil and the longitudinal distribution of the oil throughout the river at the end of the simulation (and therefore the location of the mass centroid of the oil) were nearly identical (Table 3). The resulting longitudinal

Table 3. Percentage of oil that has settled out of the water column after 5 h of simulation time and the mass centroid of the settled OPAs for all three density cases tested in the study

Oil density (kg/m^3)	Parameter	0.2 m/s	0.3 m/s	0.4 m/s	0.5 m/s	0.6 m/s	0.7 m/s
890	Oil that has settled (%)	0	2.0	24.7	47.0	68.0	68.1
	Centroid of settled OPAs (m)	N/A	5,467.0	2,684.1	1,249.6	1,150.4	592.4
968	Oil that has settled (%)	0	0.5	35.3	51.3	68.0	68.1
	Centroid of settled OPAs (m)	N/A	5,080.0	2,975.1	1,589.0	1,145.0	593.1
1,000	Oil that has settled (%)	0	0.06	21.3	47.1	68.0	68.1
	Centroid of settled OPAs (m)	N/A	5,387.0	2,800.6	1,172.9	1,171.6	582.7

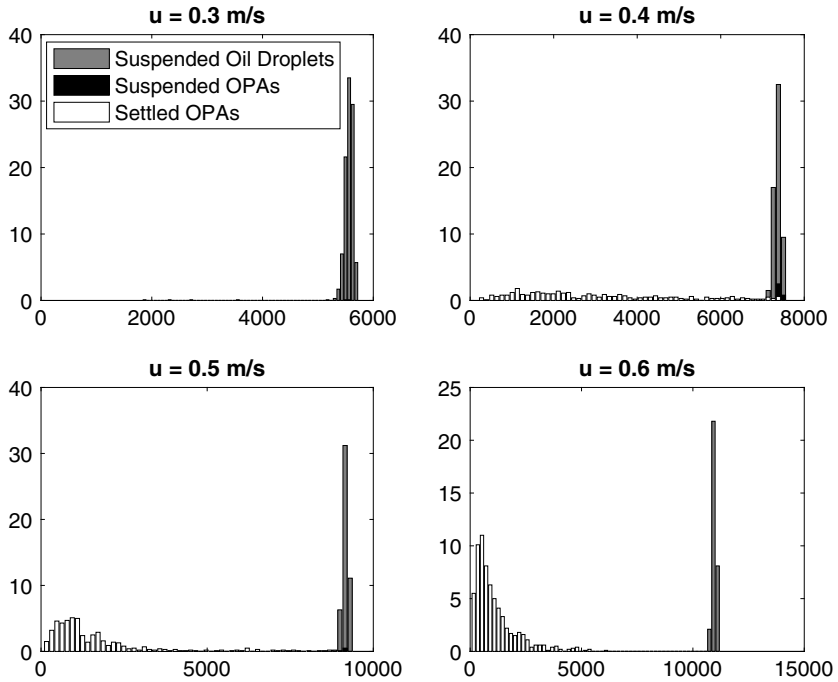

Fig. 6. Distribution of suspended oil droplets, suspended OPAs, and settled OPAs after 5 h for four different longitudinal velocities using South Louisiana crude oil.

distributions of the oil droplets and OPAs after 5 h for flow velocities of 0.3–0.6 m/s for the light oil case (a density of 820 kg/m^3) are shown in Fig. 6.

The observation that the amount of settled oil did not depend on the oil density indicates that the amount of oil that settles out of the water column is mostly dependent on the river hydraulics, sediment grain size, and the distribution of the oil droplet sizes; the density of the oil does not have a large effect. This claim is shown in Fig. 7, in which the amount of settled oil is shown to dramatically vary with velocity, but the oil density has no dominant effect. Fig. 7 also shows that, for a set of given river parameters and an oil droplet size distribution, the fraction of settled oil appears to reach an asymptote of approximately 68% when the flow velocity is equal to about 0.6 m/s.

As shown in Fig. 6 and Table 3, with an increase in the flow velocity in the river, a greater percentage of oil settles out of the water column after 5 h. As flow velocity increases, the location of the mass centroid of the settled oil decreases (Table 3). This observation indicates that as the velocity increases, the oil settles out of the water column faster, resulting in greater amounts of oil settled out further upstream. The particles' settling faster with higher flows is likely due to greater shear velocities that result from higher flows, resulting in more entrainment of sediment from the bed [Eqs. (18) and (19)], which in turn results in faster formation of the negatively buoyant OPAs. The change in the suspended

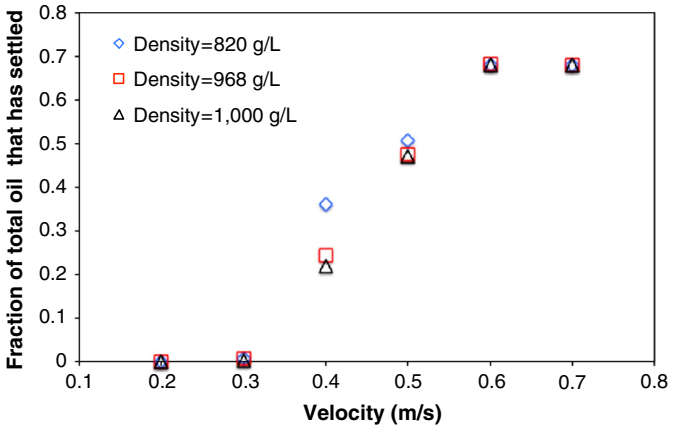

Fig. 7. Relationship of the percentage of settled oil with increased flow velocity for the three different oil densities tested.

sediment concentration profile with increasing flow velocity is shown in Fig. 8, in which greater flow velocities result in much more sediment entrained from the bed.

Another mechanism that may play an important role in how fast the OPAs form is the vertical eddy diffusivity, which is also

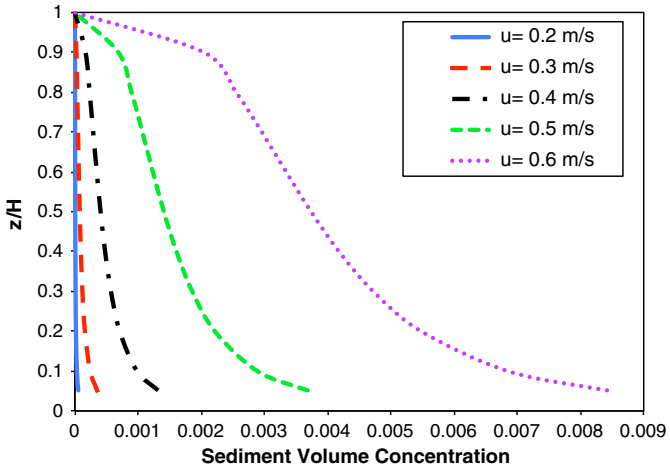

Fig. 8. Suspended sediment concentration profiles for five different velocities used in this study using a sediment grain size of 50 μm.

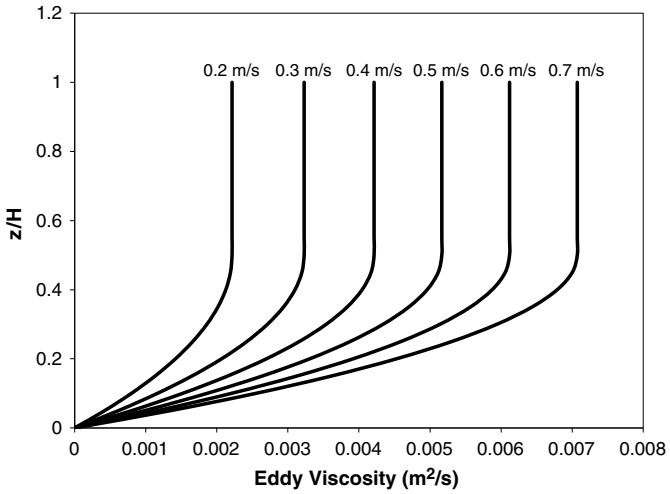

Fig. 9. Vertical fluid eddy viscosity profiles for flow velocities ranging from 0.2 to 0.7 m/s.

dependent on the shear velocity. The vertical eddy diffusivity is equal to the fluid eddy viscosity multiplied by a factor that describes the difference in the diffusion between the oil and water [Eq. (6)]. This factor takes a value between approximately 1 and 3. Since the shear velocity increases with an increase in the flow velocity, the profile of the fluid eddy viscosity also increases with the flow velocity (Fig. 9). The profiles in Fig. 9 are representative of the vertical eddy diffusivity profiles if the diffusion factor is equal to 1. The profiles, notably the constant values in the upper half of the water column, increase linearly with the flow velocity. The increase in the vertical eddy diffusivity leads to increased entrainment of the oil droplets from the surface of the water (greater movement in the vertical direction) and thus facilitates quicker formation of the OPAs.

Sensitivity Analysis

Two of the major parameters input into the model are the grain size of the sediment in the river and the total elapsed time. To quantify the impact that these parameters have on the results from the model, a sensitivity analysis is performed for these two parameters.

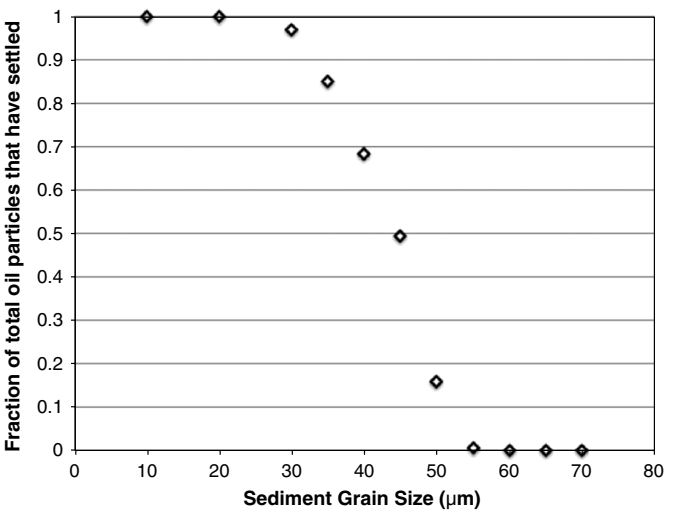

Fig. 10. Amount of settled oil as a function of the sediment grain size.

For the sediment grain size analysis, the input parameters are the same as the light oil, 0.3-m/s flow velocity case. For the elapsed time analysis, the input parameters are the same as the light oil, 0.4-m/s case.

Sediment Size

To understand the influence of the grain size of the sediment in the river, the fraction of the total amount of oil that settles after 5 h is plotted against the grain size of the sediment (Fig. 10). As can be seen in Fig. 10, the amount of settled oil is very sensitive to the grain size of the sediment, with a small change in the sediment size resulting in a great change in the amount of settled oil for sediment sizes in the range of 20–50 μm. For sediment sizes below 20 μm, all of the oil settles out of the water column, and for sediment sizes above 50 μm, none of the oil settles out of the water column. This relationship indicates not only that the model is sensitive to the sediment grain size, but also that the amount of settled oil has a carrying capacity relationship based on the sediment grain size. As discussed previously, this behavior is due to the amount of sediment that will become suspended into the water column. A smaller grain size means much more suspended sediment than a larger grain size at the same flow velocity; the drastic change in the suspended sediment concentration profiles with a change in the sediment grain size is shown in Fig. 11.

Total Elapsed Time

As the oil is transported downstream in the river for a longer period of time, it is expected that more oil will settle out of the water column. To understand the relationship between the time elapsed and the model results, the total simulation time was varied and the fraction of the total amount of oil that settles is shown in Fig. 12. As expected, as the time elapsed increases, more oil settles out of the water column. Increasing the simulation time past 6 h results in a slower increase of settled oil, suggesting that there may exist an upper limit on the amount of oil that is able to settle out of the water column with a given a set of hydraulic parameters.

Linking to a Hydraulic Model and a Case Study of the Kalamazoo River

The model described in this paper assumes a simplified, rectangular river geometry with steady, uniform flow. This simplifying assumption was used to explore how different river parameters affect OPA formation and fate; however, this limits the model to not

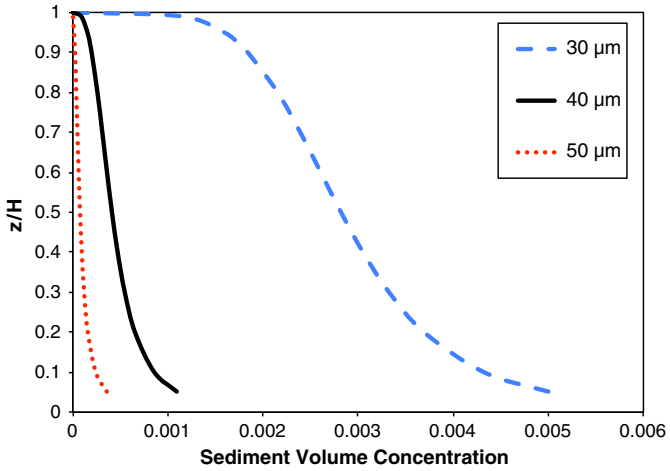

Fig. 11. Suspended sediment concentration profiles for three different sediment grain sizes using a flow velocity of 0.3 m/s.

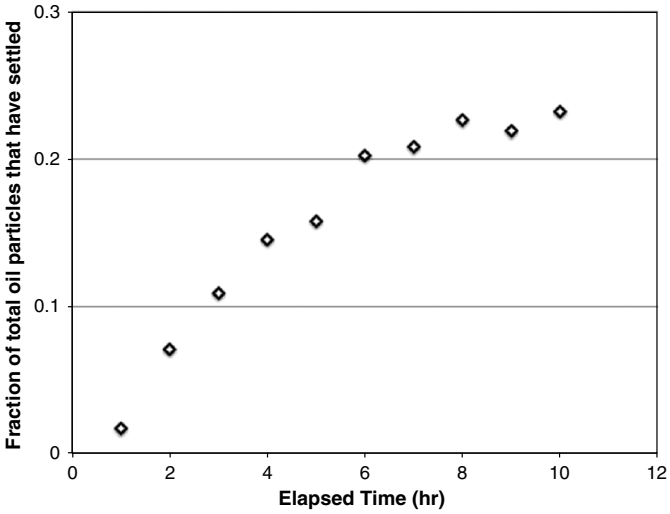

Fig. 12. Fraction of the total introduced oil that settled as a function of the elapsed time.

being applicable to real rivers with many tributary inflows and irregular geometries that cannot be approximated by a rectangular domain. To extend the use of the OPA formation and transport model to more realistic scenarios, the model was altered to accept results from a steady-flow Hydrologic Engineering Center's River Analysis System (HEC-RAS) simulation. This allows the model to describe the formation and transport of OPAs in any river geometry with spatially (but not temporally) varying flows. With this modification, the river geometry, flow velocities, water surface elevations, and bottom shear stresses along the river reach are all extracted from the HEC-RAS simulation and used to describe the river hydraulics in the OPA tracking model.

Kalamazoo River HEC-RAS Model

A HEC-RAS model of the Kalamazoo River developed by the USGS, extending from Marshall to Battle Creek, Michigan, was used for this case study (Hoard et al. 2010). The HEC-RAS model extends from the USGS Kalamazoo River gauge at Marshall, Michigan (USGS Station 04103500), to the USGS Kalamazoo River gauge near Battle Creek, Michigan (USGS Station 04105500) (Fig. 13). The structures included in the HEC-RAS model are 16 bridges, 2 dams, and 1 culvert. The bed elevation profile of the river from Marshall to Battle Creek, Michigan, is shown in Fig. 14. The two steep elevation drops are the locations of the Ceresco Dam (at approximately 9.2 km downstream of Marshall) and the Monroe St. Dam (at approximately 24.3 km downstream of Marshall).

The oil spill happened in Talmadge Creek (a tributary to the Kalamazoo River). In the HEC-RAS model, the spill is simulated as happening at the confluence of Talmadge Creek and the Kalamazoo River, since this is the location where the oil entered the Kalamazoo (Fig. 13). The length of the reach of the Kalamazoo from Marshall to Battle Creek is approximately 26.8 km, and the confluence of Talmadge Creek with the Kalamazoo is approximately 3.2 km downstream of the Marshall gauge.

The case study of the Kalamazoo presented here uses the peak flow conditions of the flood event that happened on July 25, 2010, when the rupture of the Enbridge pipeline occurred. The flood event was estimated by the USGS to be approximately a 25-year event, with the discharge in the stretch of the Kalamazoo River from Marshall to Battle Creek, shown in Fig. 15 (AECOM 2011). The discharge increases from approximately 50 m^3/s at Marshall to approximately 86 m^3/s at Battle Creek due to inflow from various tributaries. The boundary conditions used in the model are rating curves developed by the USGS at the respective USGS stream gauges. The upstream rating curve for the Marshall gauge station (USGS 04103500) is shown in Fig. 16, and the downstream rating curve for the Battle Creek gauge station (USGS 04105500) is shown in Fig. 17 (AECOM 2011).

The type of oil that entered the Kalamazoo River in 2010 was the Cold Lake Blend diluted bitumen (dilbit). Since the oil was spilled in Talmadge Creek and not directly into the Kalamazoo River, it is likely that weathering of the dilbit took place before it entered into the river. Thus, the parameters of the dilbit at 17.4% mass loss, which is the maximum weathering that took place in a study conducted by Waterman and Garcia (2015), were used. The 17.4% mass loss dilbit has a density of 992.6 kg/m^3, and the droplet size distribution shown in Fig. 18, which was determined by Waterman and Garcia (2015) via orbital shaker experiments at 180 rpm, which was found to be representative of the mixing energy of open-channel flows. Four thousand oil droplets were introduced into the river at the time of the spill, and a sediment size of 30 μm was used (which is approximately the D_{50} of the sediment in the Kalamazoo River).

Submerged Oil Assessment of the Kalamazoo River

Shortly after the oil spill into the Kalamazoo River occurred, an assessment to record the presence of submerged oil in the river was conducted (EPA 2016). From August 29 to October 29, 2010, in-channel sediment poling was conducted (EPA 2016). This poling assessment resulted in approximately 3,700 points along the river, where the number of observed OPAs were placed into four categories: none (zero OPAs), slight (one to nine OPAs), moderate (10–20 OPAs), and heavy (greater than 20 OPAs) (EPA 2016). The approximate longitudinal distribution of settled OPAs from the spill site to Battle Creek constructed from the submerged oil assessment is shown in Fig. 19. This figure shows that there were three main areas where significant submerged oil was identified: in the first 3-km stretch downstream of the spill site, at the site directly downstream of the Ceresco Dam (located approximately 10 km downstream of the spill site), and at the site directly downstream of the Monroe St. Dam (located approximately 25 km downstream of the spill site).

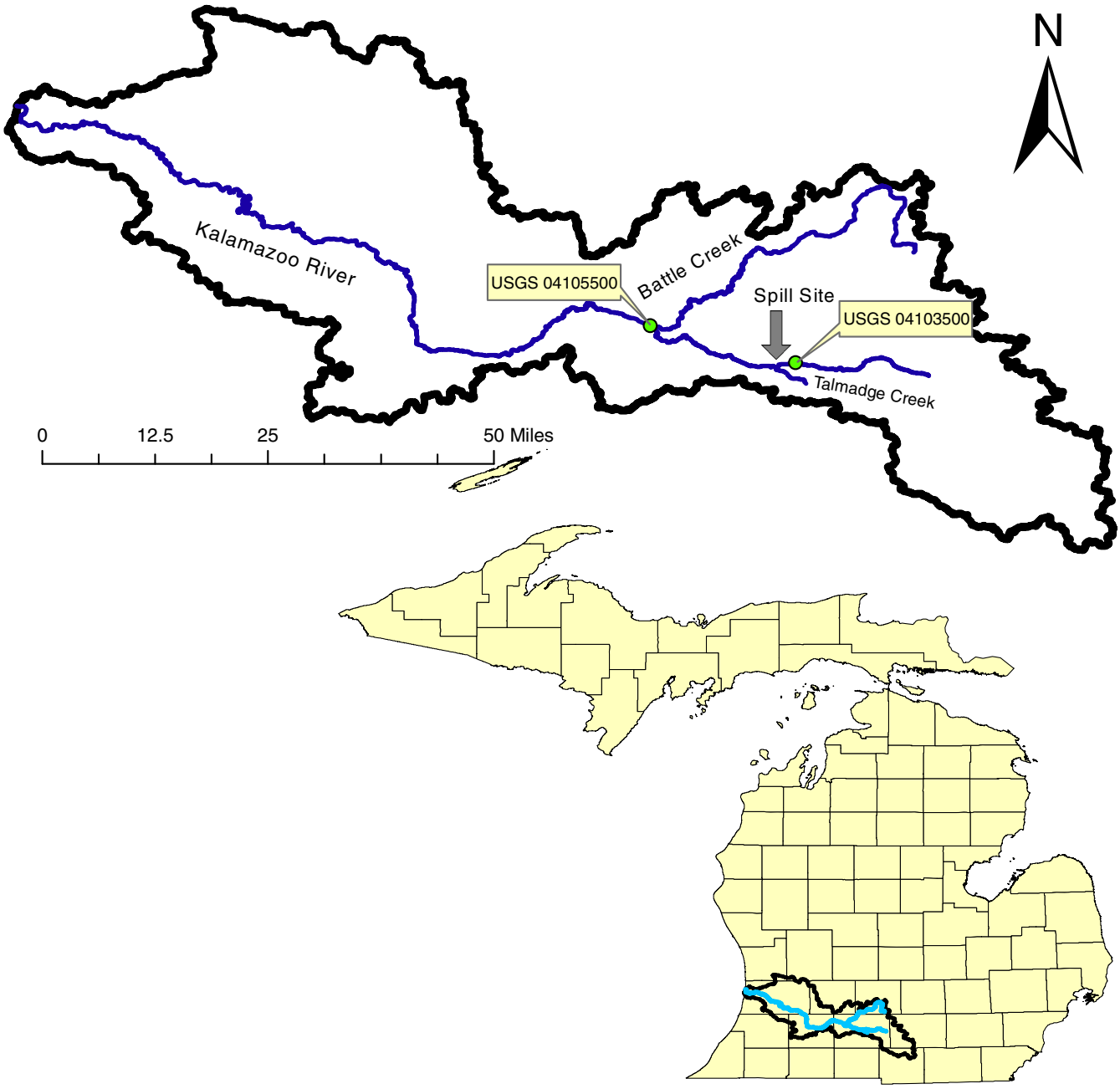

Fig. 13. Location of the Kalamazoo River in Michigan and the Kalamazoo River shown with Battle Creek and Talmadge Creek. The USGS gauges used as the upstream and downstream boundary conditions in the HEC-RAS model are marked. The spill site, which is modeled as the confluence between Talmadge Creek and the Kalamazoo River, is also marked.

Kalamazoo Case Study Results and Discussion

The leading edge of the oil droplet and OPA plume reached Battle Creek after approximately 2.6 h. The longitudinal distribution of the settled oil at the end of the 2.6-h simulation is shown in Fig. 20. In the simulation, almost all of the settled oil is located in the first 1-km stretch downstream of the spill site. While the simulation captured the large amount of settled oil that takes place directly downstream of the spill location, the areas of settled oil directly downstream of the Ceresco and Monroe St. Dams that were observed from the poling assessment in 2010 (Fig. 19) were not captured by the model. The model's inability to reproduce the 2010 poling assessment is likely due to the following reasons:

1. The particle tracking model described in this paper assumes that the oil slick is already broken into oil droplets at the beginning of the simulation; in reality, oil droplets break off from the oil slick because of turbulence and the oil–water surface tension. Thus, in the actual scenario of an oil spill, the oil droplets enter into the river domain at different times and locations, which would result in OPAs being formed later and farther downstream. In the case of the Kalamazoo River, it is likely that, as the oil slick traveled to the dams, an increase in oil droplet formation occurred because of increased levels of turbulence, which resulted in an increase in the subsequent OPA formation and settling at those locations.
2. The particle tracking model does not include effects of OPA resuspension because of lack of information on the subject. With resuspension effects included, the OPAs would have the chance to be transported farther downstream.

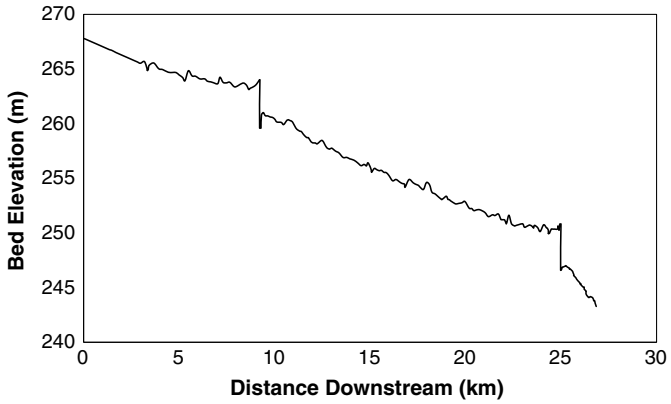

Fig. 14. Bed elevation profile of the Kalamazoo River from Marshall to Battle Creek, Michigan. The two steep drops are the locations of the Ceresco Dam (9.2 km downstream) and the Monroe St. Dam (24.3 km downstream).

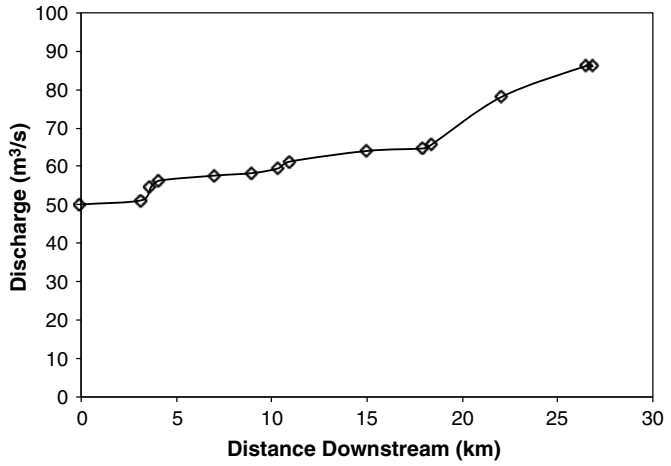

Fig. 15. Discharge along the river from Marshall to Battle Creek, Michigan, for the storm event on July 25, 2010.

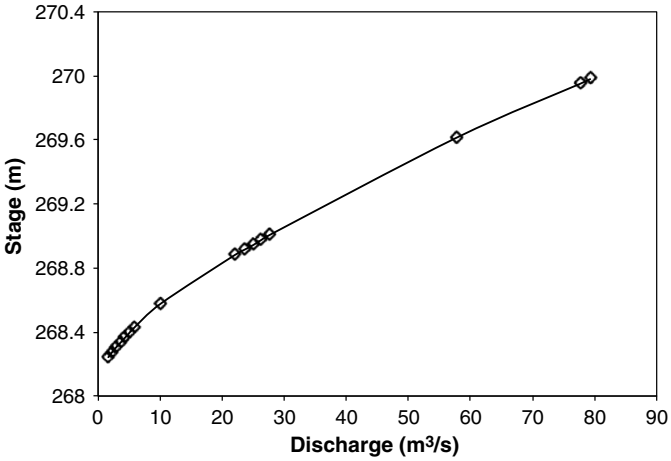

Fig. 16. Rating curve developed by the USGS at the Marshall gauge (USGS 04103500) and used as the upstream boundary condition in the HEC-RAS model.

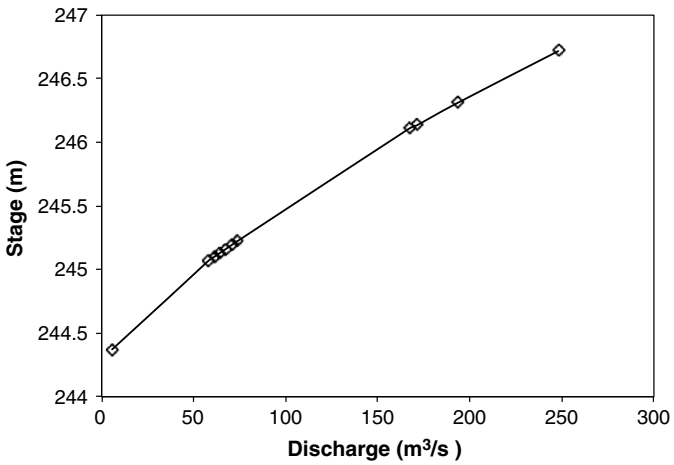

Fig. 17. Rating curve developed by the USGS at the Battle Creek gauge (USGS 04105500) and used as the downstream boundary condition in the HEC-RAS model.

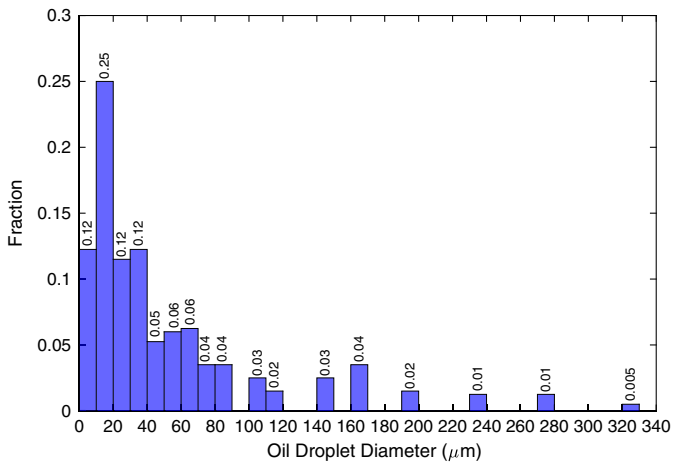

Fig. 18. Oil droplet size distribution for the dilbit with 17.4% mass loss.

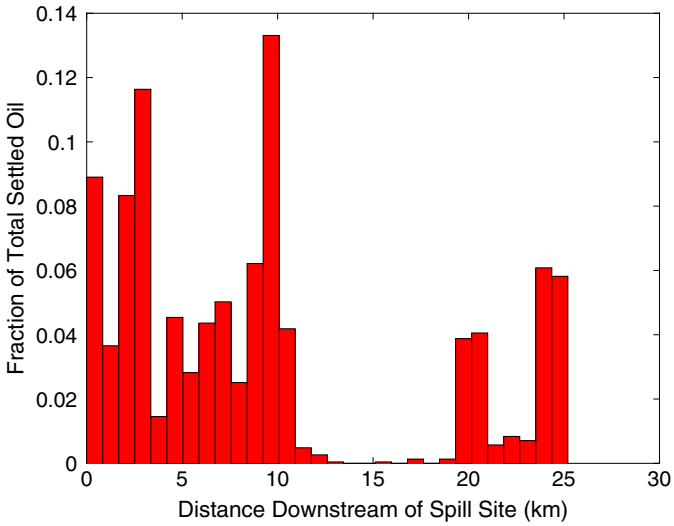

Fig. 19. Approximate longitudinal distribution of settled OPAs from the spill site to Battle Creek, constructed from the 2010 poling assessment.

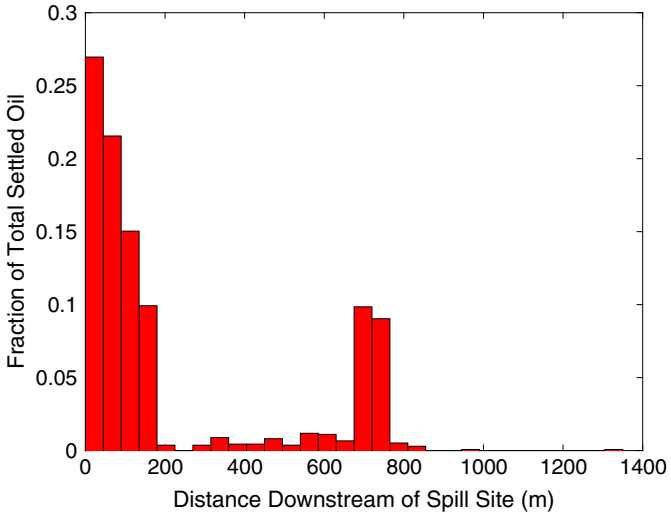

Fig. 20. Longitudinal distribution of settled particles in the Kalamazoo River simulation.

3. The poling assessment was taken 1–3 months after the oil spill occurred. It is likely that the distribution of settled oil constructed from the poling assessment (Fig. 19) is not the actual distribution of settled oil that occurred immediately after the spill.

The application of the OPA formation and transport model to the Kalamazoo River indicated that it is necessary to include the break off of oil droplets from the oil slick and resuspension of OPAs from the bed into the model in order to become a useful and deployable tool in the event of an oil spill. However, this case study provided a useful proof of concept of linking the OPA formation and transport model to HEC-RAS and identified the main areas of improvement needed to become a useful response tool.

Conclusions

A one-dimensional particle tracking model that accounts for the formation, transport, and fate of OPAs in a riverine environment was developed, validated, and tested in this study. It was shown that the flow velocity is a major parameter in determining how fast the droplets will form OPAs and settle out of the water column. With an increased flow velocity, the oil tends to settle out of the water column faster because of the increase in the suspended sediment concentration. The amount of oil that settles to the bottom of the river is also significantly dependent on the sediment grain size. The amount of settled oil behaves in a carrying capacity relationship with the sediment diameter, with all of the oil settling if the sediment is very small and none of the oil settling when the sediment size is too large. The density of the oil was shown to not meaningfully affect the amount of oil that settles out of the water column.

The particle tracking model was then linked to HEC-RAS, giving the model the ability to simulate the formation and settling of OPAs in a river domain with irregular geometry and spatially varying flows. The application to the 2010 oil spill in the Kalamazoo River provided a proof of concept for the HEC-RAS linked particle tracking model and insight into the need to include effects of oil droplet break off from the main oil slick and resuspension of settled OPAs from the bottom of the river. With this future work identified, the current model provides a robust framework for a rapid response tool in which the needed mechanisms of oil breakup and resuspension can be integrated. However, given a known type of oil, the characteristic grain size of the sediment in the river, and flow conditions during a given oil spill event, this model provides a first attempt at describing the transport of oil droplets in a riverine environment that also captures the oil droplet and sediment particle interactions. Once the identified improvements are made to this model, it has the potential to grow into a useful screening model of where settled oil is located downstream of an oil spill location, which will be able to greatly aid in oil cleanup efforts.

Acknowledgments

This material is based on work supported by the National Science Foundation Graduate Research Fellowship Program under Grant No. DGE-1144245. Additional funding for this project was provided by the EPA, Office of Research and Development (ORD), Regional Applied Research Effort Program, USGS Interagency Agreement DW-014-92452901-0. We thank Susan Mravik (EPA project officer) and Faith Fitzpatrick (USGS project manager). Useful comments by Michel Boufadel helped in improving an earlier version of this paper.

Notation

The following symbols are used in this paper:

$A = 7.8 \times 10^{-7}$;
C = volume concentration of suspended sediment;
C_b = near-bed concentration of sediment;
C_D = drag coefficient;
C_L = constant equal to 5.5;
Co = Courant number;
D_m = size of OPA when the maximum number of sediment particles are attached;
D_{oil} = diameter of oil droplet;
D_{OPA} = diameter of OPA;
D_{sed} = diameter of sediment particles;
F_{SP} = factor that accounts for effects that particle shape and packing has on coagulation;
g = acceleration of gravity;
H = water depth;
K_H = longitudinal and lateral turbulent diffusion;
K_v = vertical eddy diffusivity;
L = characteristic length of the river;
$N(D_p, t)$ = number of sediment particles attached to OPA at time t;
N_p = number of sediment particles attached to oil droplet;
N_{phex} = maximum number of sediment particles that can attach to oil droplet;
N_{sed} = number of sediment particles at oil droplet or OPA's location in water column;
R = submerged specific gravity of sediment;
R_f = empirically determined relationship given by Dietrich (1982);
R_{OPA} = Reynolds number of OPA;
R_{oil} = Reynolds number of oil droplet;
R_p = Reynolds number of sediment particle;
R_p = normally distributed random variable with mean value of zero and standard deviation of 1;
u = longitudinal velocity;
u_* = shear velocity;

u_{*s} = shear velocity multiplied by square root of fraction of shear stress that is skin friction;
$V_{\mathrm{OPA,max}}$ = maximum possible volume of OPA;
V_o = volume of oil droplet;
$V_{s,\mathrm{OPA}}$ = fall velocity of OPA;
$V_{s,\mathrm{oil}}$ = fall velocity of oil droplet;
V_{si} = fall velocity of particle with diameter of D_i;
V_{sj} = fall velocity of particle with diameter D_j;
V_{sed} = fall velocity of sediment;
v = lateral velocity;
w = vertical velocity;
x_t = x location of particle at time t;
y_t = y location of particle at time t;
$x_{t+\Delta t}$ = x location of particle at time $t + \Delta t$;
$y_{t+\Delta t}$ = y location of particle at time $t + \Delta t$;
Z = dimensionless sediment entrainment term;
z = vertical distance above bed;
z_t = z location of particle at time t;
$z_{t+\Delta t}$ = z location of particle at time $t + \Delta t$;
α = ratio of amount of successful coagulation events to total number of collisions;
α_{sta} = stability ratio;
β = collision frequency term between two particles of diameters D_i and D_j;
β_{ds} = collision frequency term due to differential settling;
β_{sh} = collision frequency term due to turbulent shear;
β_T = dimensionless factor used to describe difference in diffusion of oil droplet or OPA and fluid particle;
ΔF = dimensionless term that describes change in free energy per unit surface area of particle per unit interfacial tension between oil and water;
$\Delta N_p(t)$ = change in number of sediment particles attached to oil droplet at time t;
Δt = time step;
ζ = vertical location above bed normalized to water depth;
ζ_b = vertical location above bed where near-bed sediment concentration occurs normalized to water depth;
θ = three-phase contact angle;
κ = von Karman constant;
ν = kinematic viscosity;
π = mathematical constant pi, approximately 3.14159;
ρ_{OPA} = density of OPA;
ρ_{oil} = density of oil droplet;
ρ_w = density of fluid;
υ_T = eddy viscosity; and
ε = energy dissipation rate.

References

AECOM. 2011. *Kalamazoo River flood inundation mapping hydraulics: Technical memorandum*. Grand Rapids, MI: AECOM.

Bandara, U., P. Yapa, and H. Xi. 2011. "Fate and transport of oil in sediment laden marine waters." *J. Hydro-Environ. Res.* 5 (3): 145–156. https://doi.org/10.1016/j.jher.2011.03.002.

Dalyander, P. S., J. W. Long, N. G. Plant, and D. M. Thompson. 2014. "Assessing mobility and redistribution patterns of sand and oil agglomerates in the surf zone." *Mar. Pollut. Bull.* 80 (1): 200–209. https://doi.org/10.1016/j.marpolbul.2014.01.004.

Dietrich, W. 1982. "Settling velocity of natural particles." *Water Resour. Res.* 18 (6): 1615–1626. https://doi.org/10.1029/WR018i006p01615.

Dollhopf, R. H., F. A. Fitzpatrick, J. W. Kimble, D. M. Capone, T. P. Graan, R. B. Zelt, and R. Johnson. 2014. "Response to heavy, non-floating oil spilled in a Great Lakes river environment: A multiple-lines-of-evidence approach for submerged oil assessment and recovery." In *Proc., Int. Oil Spill Conf.*, 434–448. Washington, DC: International Oil Spill Conference.

DOT. 2017. "Table 1-10: U.S. oil and gas pipeline mileage." Accessed May 21, 2017. https://www.bts.gov/archive/publications/national_transportation_statistics/table_01_10.

EPA. 2016. *FOSC Desk Rep. for the Enbridge line 6B Oil Spill Marshall, Michigan*. Washington, DC: EPA.

EPA. 2017. "EPA response to Enbridge spill in Michigan." Accessed November 1, 2017. https://www.epa.gov/enbridge-spill-michigan.

Fischer, H. B., E. List, R. Koh, J. Imberger, and N. Brooks. 1979. *Mixing in inland and coastal waters*. New York: Academic Press.

Fitzpatrick, F. A., et al. 2015a. *Oil–particle interactions and submergence from crude oil spills in marine and freshwater environments: Review of the science and future science needs*. USGS Open-File Rep. 2015-1076. Washington, DC: USGS.

Fitzpatrick, F. A., et al. 2015b. "Integrated modeling approach for fate and transport of submerged oil and oil–particle aggregates in a freshwater riverine environment." In *Proc., SEDHYD2015 Conf.* Washington, DC: Federal Interagency Subcommittees on Hydrology and Sedimentation.

Garcia, T., P. R. Jackson, E. A. Murphy, A. J. Valocchi, and M. H. Garcia. 2013. "Development of a fluvial egg drift simulator to evaluate the transport and dispersion of Asian carp eggs in rivers." *Ecol. Modell.* 263 (1): 211–222. https://doi.org/10.1016/j.ecolmodel.2013.05.005.

García, M., and G. Parker. 1991. "Entrainment of bed sediment into suspension." *J. Hydraul. Eng.* 117 (4): 414–435. https://doi.org/10.1061/(ASCE)0733-9429(1991)117:4(414).

García, M., and G. Parker. 1993. "Experiments on the entrainment of sediment into suspension by a dense bottom current." *J. Geophys. Res. Oceans* 98 (C3): 4793–4807. https://doi.org/10.1029/92JC02404.

García, M. H. 2008. "Manual of Engineering Practice 110: Sedimentation engineering: Processes, measurements, modeling and practice." In *Proc., World Environmental and Water Resource Congress 2006: Examining the Confluence of Environmental and Water Concerns*, 1150. Reston, VA: ASCE.

Gong, Y., X. Zhao, Z. Cai, S. O'Reilly, X. Hao, and D. Zhao. 2014. "A review of oil, dispersed oil and sediment interactions in the aquatic environment: Influence on the fate, transport and remediation of oil spills." *Mar. Pollut. Bull.* 79 (1–2): 16–33. https://doi.org/10.1016/j.marpolbul.2013.12.024.

Great Lakes Commission. 2015. *Issues and trends surrounding the movement of crude oil in the Great Lakes–St. Lawrence River region*. Ann Arbor, MI: Great Lakes Commission.

Gustitus, S. A., and T. B. Clement. 2017. "Formation, fate, and impacts of microscopic and macroscopic oil–sediment residues in nearshore marine environments: A critical review." *Rev. Geophys.*, 55 (4): 1130–1157. https://doi.org/10.1002/2017RG000572.

Hayter, E., R. McCulloch, T. Redder, M. Boufadel, R. Johnson, and F. Fitzpatrick. 2015. *Modeling the transport of oil particle aggregated and mixed sediment in surface waters*. ERDC Technical Rep. Vicksburg, MS: USACE.

Hoard, C., K. Fowler, M. Kim, C. Menke, S. Morlock, M. Peppler, C. Rachol, and M. Whitehead. 2010. *Flood-inundation maps for a 15-mile reach of the Kalamazoo River from Marshall to Battle Creek, Michigan*. Scientific Investigations Map 3135. Washington, DC: USGS.

Khelifa, A., P. S. Hill, and K. Lee. 2005a. "The role of oil–sediment aggregation in dispersion and biodegradation of spilled oil." Chap. 10 in *Oil pollution and its environmental impact in the Arabian Gulf region*. Edited by M. Al-Asab, W. El-Shorbagy, and S. Al-Ghais, 131–145. Amsterdam, Netherlands: Elsevier.

Khelifa, A., P. S. Hill, and K. Lee. 2005b. "A comprehensive numerical approach to predict oil–mineral aggregate (OMA) formation following oil spills in aquatic environments." In *Proc., Int. Oil Spill Conf.*, 873–877. Washington, DC: American Petroleum Institute.

Lee, K. 2002. "Oil–particle interactions in aquatic environments: Influence on the transport, fate, effect and remediation of oil spills." *Spill Sci.*

Technol. Bull. 8 (1): 3–8. https://doi.org/10.1016/S1353-2561(03)00006-9.

Nezu, I. 2005. "Open-channel flow turbulence and its research prospect in the 21st century." *J. Hydraul. Eng.* 131 (4): 229–246. https://doi.org/10.1061/(ASCE)0733-9429(2005)131:4(229).

Rouse, H. 1939. "Experiments on the mechanics of sediment suspension." In *Proc., 5th Int. Congress on Applied Mechanics*, 550–554. Cambridge, New York: Wiley.

Singh, S. 2012. "Experiments in hydraulic engineering." In *Velocity distribution in channels*. Delhi, India: PHI Learning.

Sun, J., A. Khelifa, X. Zheng, Z. Wang, L. L. So, S. Wong, C. Yang, and B. Fieldhouse. 2010. "A laboratory study on the kinetics of formation of oil–suspended particulate matter aggregates using the NIST-1941b sediment." *Mar. Pollut. Bull.* 60 (10): 1701–1707. https://doi.org/10.1016/j.marpolbul.2010.06.044.

Tang, M., D. Huang, L. Huang, F. Xiang, and W. Yin. 1989. "Preliminary forecast of hydraulic characteristics test of grass, green, silver carp, bighead carp egg incubation conditions in the Three Gorges Reservoir area." [In Chinese.] *Reservoir Fish.* 4: 26–30.

Van Rijn, L. 1984. "Sediment transport. Part II: Suspended load transport." *J. Hydraul. Eng.* 110 (11): 1613–1641. https://doi.org/10.1061/(ASCE)0733-9429(1984)110:11(1613).

Visser, A. W. 1997. "Using random walk models to simulate the vertical distribution of particles in a turbulent water column." *Mar. Ecol. Prog. Ser.* 158: 275–281. https://doi.org/10.3354/meps158275.

Waterman, D., and M. Garcia. 2015. *Laboratory tests of oil–particle interactions in a freshwater riverine environment with cold lake blend weathered bitumen.* Civil Engineering Studies, Hydraulic Engineering Series No. 106. Urbana, IL: Univ. of Illinois.

Wright, S., and G. Parker. 2004. "Flow resistance and suspended load in sand-bed rivers: Simplified stratification model." *J. Hydraul. Eng.* 130 (8): 796–805. https://doi.org/10.1061/(ASCE)0733-9429(2004)130:8(796).

Yapa, P., H. Shen, and K. Angammana. 1994. "Modeling oil spills in a river-lake system." *J. Mar. Syst.* 4 (6): 453–471. https://doi.org/10.1016/0924-7963(94)90021-3.

Yoshioka, G., and M. Carpenter. 2002. "Characteristics of reported inland and coastal oil spills." In *Proc., 4th Biennial Freshwater Spills Symp.*, 1–11. Washington, DC: International Oil Spill Conference.

Zhang, H. P., M. Khatibi, Y. Zheng, K. Lee, Z. K. Li, and J. V. Mullin. 2010. "Investigation of OMA formation and the effect of minerals." *Mar. Pollut. Bull.* 60 (9): 1433–1441. https://doi.org/10.1016/j.marpolbul.2010.05.014.

Zhao, L., M. Boufadel, X. Geng, K. Lee, T. King, B. Robinson, and F. Fitzpatrick. 2016. "A-DROP: A predictive model for the formation of oil particle aggregates (OPAs)." *Mar. Pollut. Bull.* 106 (1–2): 245–259. https://doi.org/10.1016/j.marpolbul.2016.02.057.

Zhao, L., M. Boufadel, J. Katz, G. Haspel, K. Lee, T. King, and B. Robinson. 2017. "A new mechanism of sediment attachment to oil in turbulent flows: Projectile particles." *Environ. Sci. Technol.* 51 (19): 11020–11028. https://doi.org/10.1021/acs.est.7b02032.

Zhao, L., J. Torlapati, M. Boufadel, T. King, B. Robinson, and K. Lee. 2014. "VDROP: A comprehensive model for droplet formation of oils and gases in liquids: Incorporation of the interfacial tension and droplet viscosity." *Chem. Eng. J.* 253: 93–106. https://doi.org/10.1016/j.cej.2014.04.082.

Zheng, L., and P. Yapa. 2000. "Buoyant velocity of spherical and non-spherical bubbles/droplets." *J. Hydraul. Eng.* 126 (11): 852–854. https://doi.org/10.1061/(ASCE)0733-9429(2000)126:11(852).

Zhu, Z. 2015. "Modeling the transport and fate of oil–particle aggregates after an oil spill in inland waterways." Ph.D. dissertation, Dept. of Civil and Environmental Engineering, Univ. of Illinois at Urbana–Champaign.

Zhu, Z., D. Waterman, and M. Garcia. 2018. "Modeling the transport of oil–particle aggregates resulting from an oil spill in a freshwater environment." *Environ. Fluid Mech.* 18 (4): 1–10. https://doi.org/10.1007/s10652-018-9581-0.